

***s*-wave superconductivity in optimally doped SrTi_{1-x}Nb_xO₃ unveiled by electron irradiation**Xiao Lin,^{1,*} Carl Willem Rischau,^{1,2} Cornelis J. van der Beek,² Benoît Fauqué,¹ and Kamran Behnia¹¹*Laboratoire de Physique et d'Etude des Matériaux, Centre National de la Recherche Scientifique, ESPCI, UPMC, Paris F-75005, France*²*Laboratoire des Solides Irradiés, Centre National de la Recherche Scientifique, CEA, DSM, IRAMIS,**Ecole Polytechnique, 91128 Palaiseau Cedex, France*

(Received 7 July 2015; published 3 November 2015)

We report on a study of electric resistivity and magnetic susceptibility measurements in electron irradiated SrTi_{0.987}Nb_{0.013}O₃ single crystals. Pointlike defects, induced by electron irradiation, lead to an almost threefold enhancement of the residual resistivity, but barely affect the superconducting critical temperature (T_c). The pertinence of Anderson's theorem provides strong evidence for a *s*-wave superconducting order parameter. Stronger scattering leads to a reduction of the effective coherence length (ξ) and the deduced intrinsic coherence length (ξ_0) is close to the BCS coherence length (ξ_{BCS}). Combined with thermal conductivity data pointing to multiple nodeless gaps, the current results identify optimally doped SrTi_{1-x}Nb_xO₃ as a multiband *s*-wave superconductor.

DOI: [10.1103/PhysRevB.92.174504](https://doi.org/10.1103/PhysRevB.92.174504)

PACS number(s): 74.62.Dh, 74.20.-z, 74.25.fc, 74.25.Ha

I. INTRODUCTION

Scattering mixes the superconducting order parameter at separate points on the Fermi surface. As a consequence, one can probe changes in the two-particle wave function by tuning disorder. Its effect on the superconducting transition provides an opportunity to explore the symmetry of the superconducting gap. According to Anderson's theorem, in a conventional *s*-wave superconductor the critical temperature (T_c) is insensitive to nonmagnetic disorder [1]. On the other hand, in superconductors with nontrivial gap symmetry, e.g., cuprates [2–4], Sr₂RuO₄ [5], and heavy fermions [6], T_c is extremely sensitive to potential scattering and the superconducting ground state can be completely destroyed by disorder [7–10]. In multiband superconductors such as MgB₂ and iron pnictides, interband scattering rather than intraband scattering plays a key role in suppressing T_c and the effect of disorder depends on the ratio of interband to intraband scattering matrix elements [11–13].

Chemical substitution can be used to introduce disorder. In cuprates, T_c is drastically suppressed by Zn doping, providing strong evidence for *d*-wave symmetry [2]. Particle irradiation provides an alternative avenue of creating artificial defects without introducing any foreign ions. In YBa₂Cu₃O_{7- δ} , scattering induced by electron irradiation suppressed T_c in a manner similar to Zn substitution [4,14,15]. On the other hand, in the *s*-wave superconductor MgB₂, superconductivity is robust with respect to electron irradiation [16–18]. In the present paper, electron irradiation is utilized to investigate the superconducting order parameter in optimally doped SrTi_{1-x}Nb_xO₃ single crystals.

A band insulator with an energy gap of 3.2 eV, SrTiO₃ is close to a ferroelectric instability aborted due to quantum fluctuations [19]. Its huge permittivity at low temperature leads to a very long Bohr radius and a precocious metallicity. Three conducting bands originating from Ti t_{2g} orbitals and centered at the Γ point can be successfully filled by n doping [20]. A superconducting dome with a peak $T_c \simeq 450$ mK [21–25] exists between charge carrier densities of 3×10^{17} to $3 \times$

10^{20} cm⁻³. Superconductivity survives even in the extreme dilute limit with the Fermi energy (ϵ_F) lower than the Debye temperature (T_D) [23], which challenges the conventional phonon mediated weak-coupling BCS theory. Several exotic superconducting mechanisms have been proposed to explain the superconductivity in SrTiO₃ by invoking soft phonons [26], plasmons and polar optical phonons [27], and the vicinity to the ferroelectric quantum critical point [28].

The symmetry of the superconducting order parameter has been barely explored in this system. In 1980, Binnig and coauthors detected two distinct superconducting gaps by planar tunneling measurements [29]. However, a recent tunneling experiment on the superconducting LaAlO₃/SrTiO₃ interface did not detect multiple gaps [30]. More recently, thermal conductivity measurements found multiple nodeless gaps in optimally doped SrTi_{1-x}Nb_xO₃ single crystals, paving the way for the identification of the symmetry of the superconducting order parameter [31]. A recent study reported the existence of electron pairs well beyond the superconducting ground state in quantum dots fabricated on the LaAlO₃/SrTiO₃ interface [32]. In this paper, we present a study of ac susceptibility and resistivity in SrTi_{1-x}Nb_xO₃ irradiated with high-energy electrons and provide unambiguous evidence for *s*-wave superconductivity.

II. EXPERIMENTAL

The SrTi_{1-x}Nb_xO₃ ($x = 0.013$) single crystals used in this study were obtained commercially as the one used in thermal conductivity measurements [31]. Four samples with size of $5 \times 2.5 \times 0.5$ mm have been cut from the same single crystal and gold was evaporated on their surface to make Ohmic contacts. Three of them were irradiated with 2.5-MeV electrons at the SIRIUS accelerator facility of the Laboratoire des Solides Irradiés. Irradiations were performed at 20 K in liquid hydrogen to obtain a uniform distribution of point defects in the material. After irradiation, the samples were stored in liquid nitrogen to avoid room-temperature annealing of the irradiation induced defects. The resistivity and Hall effect around the superconducting transition temperature were measured with a standard four probe method in a dilution

*xiao.lin@espci.fr

refrigerator within a few days after the irradiation. The transport properties were rechecked in a Quantum Design Physical Property Measurement System (PPMS) system above 2 K a few months later. The Hall carrier density and residual resistivity have barely changed with time. Gold contacts that are large compared to the size of the samples may give rise to an uncertainty of 10% in the transport measurements. Finally, the ac susceptibility was measured in a homemade setup, which consisted of one primary field coil and one compensating pick-up coil with two subcoils with their turns in opposite directions. The exciting ac current was supplied and the induced voltage signal was picked up by a lock-in amplifier. The applied ac magnetic field was as low as 10 mG, with frequencies between 2000 and 4000 Hz.

III. RESULTS AND DISCUSSION

Figures 1(a) and 1(b) show the temperature dependence of the resistivity of the pristine sample no. 1 and of samples no. 2, no. 3, and no. 4 that were irradiated to total electron doses $Q = 300, 460,$ and 1320 mC/cm^2 respectively. Rather than modifying the room-temperature resistivity, the electron irradiation induced defect scattering clearly increases the low-temperature resistivity. The residual resistivity $\rho_0 = \rho(2 \text{ K})$

TABLE I. Irradiation dose (Q), superconducting critical temperature from ac susceptibility ($T_{c-\chi'}$) and resistivity ($T_{c-\rho}$) at zero field, residual resistivity at 2 K (ρ_0), T^2 prefactor (A), superconducting effective coherence length (ξ), and mean free path (l) for pristine and electron irradiated $\text{SrTi}_{0.987}\text{Nb}_{0.013}\text{O}_3$ single crystals.

	No. 1	No. 2	No. 3	No. 4
$Q(\text{mC/cm}^2)$	0	300	460	1320
$T_{c-\text{sus}}$ (K)	0.37	0.372	0.35	0.368
$T_{c-\rho}$ (K)	0.435	0.435	0.42	0.419
ρ_0 ($\mu\Omega \text{ cm}$)	71	100	117	173
A ($\mu\Omega \text{ cm/K}^2$)	0.048	0.049	0.051	0.043
ξ (nm)	76	74	70	59
l (nm)	51	38	31	19

amounts to $71 \mu\Omega \text{ cm}$ in the pristine sample and increases with increasing irradiation dose. Consistent with [33], all the samples present Fermi-liquid behavior with T^2 resistivity expressed by $\rho = \rho_0 + AT^2$. Listed in Table I, the T^2 prefactor A from inelastic electron scattering is around $0.048 \mu\Omega \text{ cm/K}^2$ with an error of 10%. Hence the pointlike defects induced by the electron irradiation barely affect the inelastic scattering at higher temperature, but only increase the elastic scattering at zero temperature.

Figure 1(c) plots the Hall resistivity as a function of the magnetic field at 10 K. The Hall carrier concentration (n_H) plotted in Fig. 1(d) remains around $2.1 \times 10^{20} \text{ cm}^{-3}$ with an error of 10%, deduced from $R_H = 1/n_H e$ where $R_H = \rho_{yx}/B$ is the Hall coefficient. As seen in the figure, while the carrier concentration does not show any substantial change, ρ_0 increases linearly with the irradiation dose, indicating that the magnitude of the scattering rate is affected by the increased quantity of irradiation induced scattering centers. ρ_0 amounts to $175 \mu\Omega \text{ cm}$ in sample no. 4, enhanced by $104 \mu\Omega \text{ cm}$ compared to no. 1, a magnitude comparable to what has been attained in other studies of impurity effects in superconductors such as cuprates [2] and pnictides [11]. The mean free path (l) can be extracted using $l = \hbar\mu k_F/e$, where \hbar and e are the fundamental constants, μ is the Hall mobility, and k_F is the Fermi wave factor, calculated from the carrier density assuming an isotropic single-component Fermi surface. With increasing Q , l decreases from 50 to 19 nm.

Figure 2 shows the superconducting transition in different samples such as observed through the real part of the susceptibility (χ') and the resistivity (normalized by its normal-state magnitude). There is a smooth transition in ρ/ρ_n and the resistivity vanishes at a critical temperature ($T_{c-\rho}$) of 435 mK. On the other hand, χ' monitors bulk superconductivity, i.e., full flux exclusion. The bulk superconducting transition occurs at a temperature $T_{c-\chi'}$, determined as the crossing point of two linear extrapolations, close to 370 mK. Such a difference of 65 mK between $T_{c-\rho}$ and $T_{c-\chi'}$ —comparable to what was reported in our previous study comparing the specific heat, the thermal conductivity, and the resistive superconducting transitions [31]—is not changed by point-defect disorder. As seen in the figure, both $T_{c-\rho}$ and $T_{c-\chi'}$ remain basically the same in the four samples. This is the principal result of this study. In spite of the significant decrease of the charge-carrier

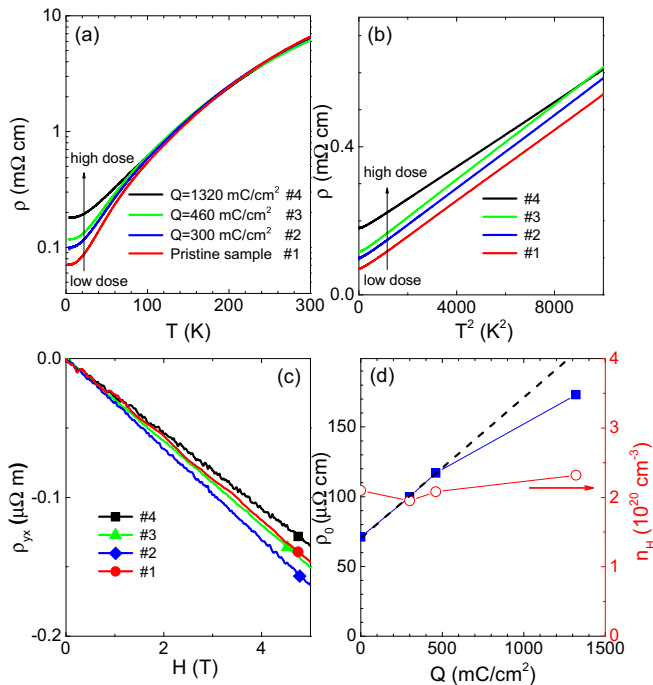


FIG. 1. (Color online) Resistivity and Hall coefficient in pristine and electron irradiated $\text{SrTi}_{0.987}\text{Nb}_{0.013}\text{O}_3$ single crystals. (a) Temperature dependence of resistivity (note the vertical log scale). The low-temperature resistivity monotonically increases with irradiation dose. (b) Resistivity as a function of T^2 . All the samples show T^2 resistivity hardly altered by electron irradiation. (c) Hall resistivity (ρ_{yx}) as a function of magnetic field at 10 K. (d) Residual resistivity [$\rho_0 = \rho(2 \text{ K})$] and Hall carrier concentration (n_H) as a function of irradiation dose (Q). Irradiation enhances the residual resistivity by a factor of 2.5, but leaves the carrier density virtually unchanged ($n_H \approx 2.1 \times 10^{20} \text{ cm}^{-3}$). The dashed line is a guide to the eyes.

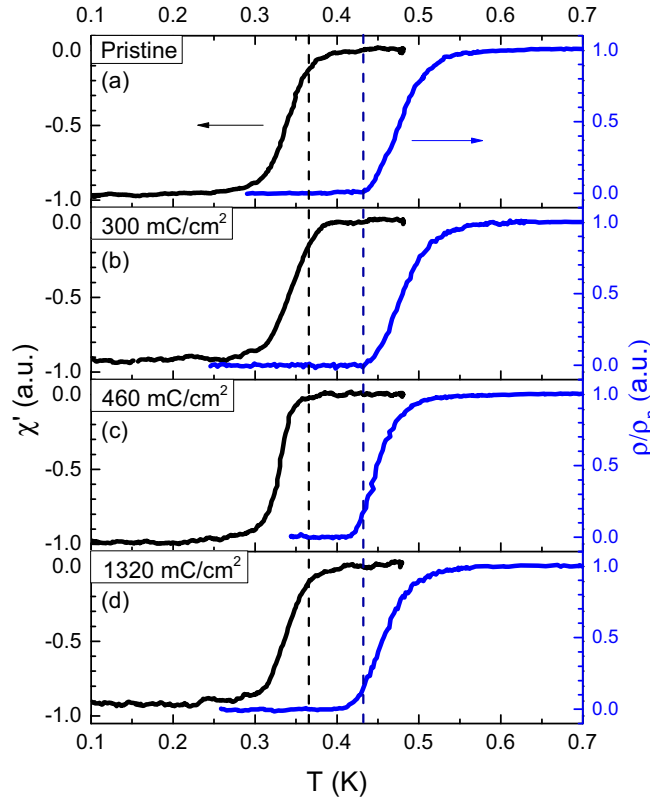


FIG. 2. (Color online) The real part of ac susceptibility (χ') and normalized resistivity (ρ/ρ_n) as a function of temperature around T_c in the absence of magnetic field for pristine and electron irradiated $\text{SrTi}_{0.987}\text{Nb}_{0.013}\text{O}_3$. Two vertical lines mark the transition temperatures in χ' and ρ/ρ_n . The superconducting transition barely shifts.

mean free path, the critical temperature remains the same. Neither the width of the transition nor the superconducting shielding fraction are affected by the irradiations. Table I lists $T_{c-\rho}$ and $T_{c-\chi'}$.

Figures 3(a) and 3(b) plot $\chi'(T)$ near T_c in the presence of a magnetic field for samples no. 1 and no. 4. As expected, the application of a magnetic field shifts the superconducting transition to lower temperatures. In Fig. 3(c), H_{c2} is plotted as a function of $T/T_c(0T)$ for all the samples. A remarkable effect of the irradiation is to induce an enhancement of the slope of the upper critical field near T_c . One can quantify this effect by extracting the effective coherence length (ξ) from this slope using the expression based on the Werthammer-Helfand-Hohenberg theory [34]:

$$1/\xi = \sqrt{\frac{2\pi\alpha}{\phi_0} T_c(0T) \left. \frac{dH_{c2}}{dT} \right|_{T=T_c(0T)}}. \quad (1)$$

Here, ϕ_0 is the flux quanta and α is a dimensionless parameter ranging from 0.725 in the clean limit to 0.69 in the dirty limit. By assuming a dirty superconductor, the effective coherence length passes from 76 nm in the pristine sample no. 1 to 59 nm in the most irradiated sample no. 4 (see Table I). Shortening the mean free path leads to a decreasing effective coherence length ξ . This is expected, since ξ can be expressed

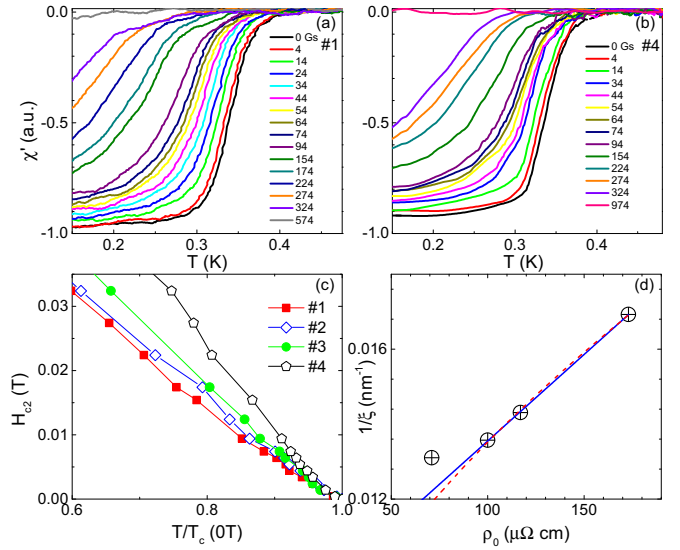


FIG. 3. (Color online) The evolution of the upper critical field (H_{c2}) and the effective coherence length (ξ) with electron irradiation. (a) and (b) χ' as a function of temperature around the superconducting transition at different magnetic fields, for samples no. 1 and no. 4, respectively. (c) The evolution of H_{c2} with $T/T_c(0T)$ from χ' . The slope of H_{c2} near T_c evolves with irradiation. (d) $1/\xi$, as extracted from the upper critical field, as a function of ρ_0 . The solid line is a linear fit from Eq. (2) and the dashed line is a fit from Eq. (3).

in BCS theory as

$$1/\xi = 1/\xi_0 + 1/\beta. \quad (2)$$

Here, ξ_0 is the intrinsic superconducting coherence length and β is the characteristic length of electrodynamic response of the normal state current. Pippard argued that the order of magnitude of β in a metal is the mean free path of electrons (l) [35,36]. Plotting $1/\xi$ as a function of ρ_0 in Fig. 3(d), one can extract an intercept, which yields $\xi_0 \sim 112$ nm. According to BCS and Ginzburg-Landau (GL) theory [36], Fig. 3(d) can alternatively be fitted by

$$1/\xi = \frac{2\sqrt{3}}{\pi} \frac{\sqrt{1 + \xi_0/l}}{\xi_0}, \quad (3)$$

yielding $\xi_0 \sim 168$ nm. Equations (2) and (3) are valid only when the vector potential (A) and the BCS or GL wave function (ψ) vary slowly over a distance of ξ . This requires ξ to be shorter than the penetration length (λ) [36]. The locality is satisfied in $\text{SrTi}_{1-x}\text{Nb}_x\text{O}_3$ in which H_{c1} is two orders of magnitude smaller than H_{c2} [37] and is strengthened by defect scattering induced by electron irradiation. From both fits, ξ_0 is close to the BCS coherence length (ξ_{BCS}), which can be estimated to be $\xi_{\text{BCS}} = \hbar v_F / \pi \Delta(0) \sim 140$ nm. The magnitude of the Fermi velocity v_F is given by $\hbar k_F / m^*$ with $m^* = 4m_e$ [31], while the superconducting gap $\Delta(0K) \sim 80 \mu\text{eV}$ is inferred from early tunneling experiments [29]. We conclude that ξ_0 is larger than the mean free path in all samples, indicating that the single crystals in this study are dirty superconductors [38].

Let us compare our results with what has been reported in the case of other superconductors. Abrikosov and Gor'kov

formulated a theory for the response of conventional superconductors to magnetic impurities [39]. According to this theory, T_c is suppressed:

$$-\ln\left(\frac{T_c}{T_{c0}}\right) = \psi\left(\frac{1}{2} + \frac{\alpha T_{c0}}{4\pi T_c}\right) - \psi\left(\frac{1}{2}\right). \quad (4)$$

Here, ψ is the digamma function, T_{c0} is the superconducting critical temperature in the clean limit, $\alpha = 2\hbar\tau_s/k_B T_{c0}$ is the dimensionless pair-breaking parameter, and τ_s is the spin-flip scattering lifetime. Equation (4) can be generalized to unconventional superconductors and their T_c evolution with nonmagnetic potential scattering. This can be done by replacing α with $\hbar\tau_p/k_B T_{c0}$, in which τ_p is the potential scattering lifetime [3,7,8]. In order to make a simple comparison between experiment and theory, we take the residual resistivity as a measure of τ_p , taken to be equal to the transport lifetime τ_{imp} , expressed by $\tau_{\text{imp}} = \frac{m^*}{\rho n e^2}$.

Figure 4 shows T_c/T_{c0} as a function of $\hbar\tau_{\text{imp}}/k_B T_{c0}$ (α) for $\text{SrTi}_{0.987}\text{Nb}_{0.013}\text{O}_3$, compared with three other superconductors. These are the conventional superconductor MgB_2 [16], as well as two unconventional superconductors $\text{YBa}_2\text{Cu}_3\text{O}_{7-\delta}$ (d -wave) [2] and Sr_2RuO_4 (p -wave) [5], which are both perovskites like the system under study. In both $\text{YBa}_2\text{Cu}_3\text{O}_{7-\delta}$ and Sr_2RuO_4 , T_c is extremely sensitive to the introduction of disorder and superconductivity is completely destroyed when α exceeds a number of the order of unity. In contrast, superconductivity in $\text{SrTi}_{0.987}\text{Nb}_{0.013}\text{O}_3$ is robust and T_c shows a negligible variation even when α becomes very large. A similar behavior was observed in MgB_2 . This is strong evidence for s -wave superconductivity in $\text{SrTi}_{0.987}\text{Nb}_{0.013}\text{O}_3$ and the main conclusion of this study.

IV. CONCLUSION

In summary, performing resistivity and ac susceptibility measurements on electron irradiated optimally doped $\text{SrTi}_{0.987}\text{Nb}_{0.013}\text{O}_3$, we have found that superconductivity is robust against impurity potential scattering deep into the dirty limit ($\xi_0/l \sim 5.9\text{--}8.8$). In addition, we have quantified the intrinsic clean coherence length (ξ_0) and found that it is comparable to the BCS coherence length (ξ_{BCS}). Combined with the thermal conductivity data, which pointed to the absence of nodal quasiparticles [31], this result identifies $\text{SrTi}_{1-x}\text{Nb}_x\text{O}_3$ as a multigap s -wave superconductor. The negligible suppression of T_c also indicates that the relative

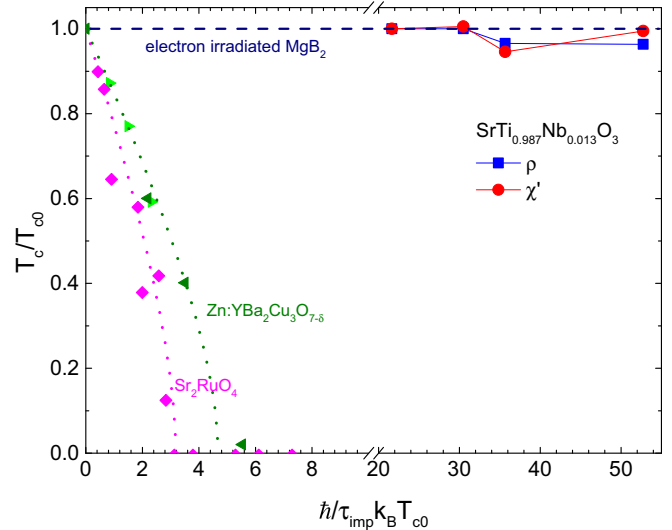


FIG. 4. (Color online) T_c/T_{c0} as a function of the dimensionless pair-breaking rate $\alpha = \hbar\tau_{\text{imp}}/k_B T_{c0}$ in $\text{SrTi}_{0.987}\text{Nb}_{0.013}\text{O}_3$ determined from resistivity (■) and ac susceptibility (●). The data for MgB_2 under electron irradiation (the horizontal dashed line) [16] are plotted for comparison, as well as those for two unconventional superconductors, Zn-doped cuprates (◄: $\text{YBa}_2\text{Cu}_3\text{O}_{6.63}$, ►: $\text{YBa}_2\text{Cu}_3\text{O}_{6.93}$) [2] and slightly disordered Sr_2RuO_4 (◆) [5]. The dotted lines are guides to the eyes. Superconductivity is robust against impurity scattering in $\text{SrTi}_{0.987}\text{Nb}_{0.013}\text{O}_3$ and in MgB_2 , but is rapidly suppressed in the two unconventional superconductors.

weight of interband and intraband scattering is not altered by electron irradiation. In oxygen deficient SrTiO_3 with a carrier concentration 400 times lower than the samples studied here, the Fermi energy becomes one order of magnitude lower than the Debye temperature, a serious challenge for a phonon-mediated pairing mechanism [23]. Further experiments are required to probe the evolution of the gap symmetry and the pairing mechanism in a system whose superconductivity survives over three orders of magnitude of carrier concentration.

ACKNOWLEDGMENTS

We thank the staff of the SIRIUS accelerator for technical support. This work is supported by Agence Nationale de la Recherche as part of SUPERFIELD and QUANTUM LIMIT projects.

- [1] P. W. Anderson, *J. Phys. Chem. Solids* **11**, 26 (1959).
- [2] Y. Fukuzumi, K. Mizuhashi, K. Takenaka, and S. Uchida, *Phys. Rev. Lett.* **76**, 684 (1996).
- [3] S. K. Tolpygo, J.-Y. Lin, and M. Gurvitch, S. Y. Hou, and J. M. Phillips, *Phys. Rev. B* **53**, 12454 (1996).
- [4] F. Rullier-Albenque, P. A. Vieillefond, H. Alloul, A. W. Tyler, P. Lejay, and J. F. Marucco, *Europhys. Lett.* **50**, 81 (2000).
- [5] A. P. Mackenzie and Y. Maeno, *Rev. Mod. Phys.* **75**, 657 (2003).
- [6] J. S. Kim, D. Bedorf, and G. R. Stewart, *J. Low Temp. Phys.* **157**, 29 (2009).
- [7] R. J. Radtke, K. Levin, H. B. Schüttler, and M. R. Norman, *Phys. Rev. B* **48**, 653 (1993).
- [8] A. A. Abrikosov, *Physica C* **214**, 107 (1993).
- [9] A. J. Millis, S. Sachdev, and C. M. Varma, *Phys. Rev. B* **37**, 4975 (1988).
- [10] L. S. Borkowski, and P. J. Hirschfeld, *Phys. Rev. B* **49**, 15404 (1994).
- [11] R. Prozorov, M. Kończykowski, M. A. Tanatar, A. Thaler, S. L. Budko, P. C. Canfield, V. Mishra, and P. J. Hirschfeld, *Phys. Rev. X* **4**, 041032 (2014).
- [12] A. A. Golubov and I. I. Mazin, *Phys. Rev. B* **55**, 15146 (1997).

- [13] Y. Wang, A. Kreisel, P. J. Hirschfeld, and V. Mishra, *Phys. Rev. B* **87**, 094504 (2013).
- [14] F. Rullier-Albenque, H. Alloul, and R. Tourbot, *Phys. Rev. Lett.* **87**, 157001 (2001).
- [15] A. Legris, F. Rullier-Albenque, E. Radeva, and P. Lejay, *J. Phys. I (France)* **3**, 1605 (1993).
- [16] A. A. Blinkin, V. V. Derevyanko, A. N. Dovbnya, T. V. Sukhareva, V. A. Finkel, and I. N. Shlyakhov, *Phys. Solid State* **48**, 2037 (2006).
- [17] T. Klein, R. Marlaud, C. Marcenat, H. Cercellier, M. Konczykowski, C. J. van der Beek, V. Mosser, H. S. Lee, and S. I. Lee, *Phys. Rev. Lett.* **105**, 047001 (2010).
- [18] A. A. Blinkin, V. V. Derevyanko, T. V. Sukhareva, V. L. Uvarov, V. A. Finkel, Yu. N. Shakhov, and I. N. Shlyakhov, *Phys. Solid State* **53**, 245 (2011).
- [19] K. A. Müller and H. Burkard, *Phys. Rev. B* **19**, 3593 (1979).
- [20] D. van der Marel, J. L. M. van Mechelen, and I. I. Mazin, *Phys. Rev. B* **84**, 205111 (2011).
- [21] J. F. Schooley, W. R. Hosler, E. Ambler, J. H. Becker, M. L. Cohen, and C. S. Koonce, *Phys. Rev. Lett.* **14**, 305 (1965).
- [22] C. S. Koonce, Marvin L. Cohen, J. F. Schooley, W. R. Hosler, and E. R. Pfeiffer, *Phys. Rev.* **163**, 380 (1967).
- [23] X. Lin, Z. W. Zhu, B. Fauqué, and K. Behnia, *Phys. Rev. X* **3**, 021002 (2013).
- [24] J. F. Schooley, W. R. Hosler, and M. L. Cohen, *Phys. Rev. Lett.* **12**, 474 (1964).
- [25] X. Lin, G. Bridoux, A. Gourgout, G. Seyfarth, S. Krämer, M. Nardone, B. Fauqué, and K. Behnia, *Phys. Rev. Lett.* **112**, 207002 (2014).
- [26] J. Appel, *Phys. Rev.* **180**, 508 (1969).
- [27] Y. Takada, *J. Phys. Soc. Jpn.* **49**, 1267 (1980).
- [28] S. E. Rowley, L. J. Spalek, R. P. Smith, M. P. M. Dean, M. Itoh, J. F. Scott, G. G. Lonzarich, and S. S. Saxena, *Nature Physics* **10**, 367 (2014).
- [29] G. Binnig, A. Baratoff, H. E. Hoening, and J. G. Bednorz, *Phys. Rev. Lett.* **45**, 1352 (1980).
- [30] C. Richter, H. Boschker, W. Dietsche, E. Fillis-Tsirakis, R. Jany, F. Loder, L. F. Kourkoutis, D. A. Muller, J. R. Kirtley, C. W. Schneider, and J. Mannhart, *Nature (London)* **502**, 528 (2013).
- [31] X. Lin, A. Gourgout, G. Bridoux, F. Jomard, A. Pourret, B. Fauqué, D. Aoki, and K. Behnia, *Phys. Rev. B* **90**, 140508(R) (2014).
- [32] G. L. Cheng, M. Tomczyk, S. C. Lu, J. P. Veazey, M. C. Huang, P. Irvin, S. Ryu, H. Lee, C. B. Eom, C. S. Hellberg, and J. Levy, *Nature (London)* **521**, 196 (2015).
- [33] X. Lin, B. Fauqué, and K. Behnia, *Science* **349**, 945 (2015).
- [34] E. Helfand and N. R. Werthamer, *Phys. Rev.* **147**, 288 (1966); N. R. Werthamer, E. Helfand, and P. C. Hohenberg, *ibid.* **147**, 295 (1966).
- [35] A. B. Pippard, *Proc. R. Soc. London A* **216**, 547 (1953).
- [36] M. Tinkham, *Introduction to Superconductivity* (McGraw-Hill, New York, 1975).
- [37] E. Ambler, J. H. Colwell, W. R. Hosler, and J. F. Schooley, *Phys. Rev.* **148**, 280 (1966).
- [38] Note that the upper critical field extracted from resistivity is substantially larger than what is deduced here from the shift in the bulk transition temperature with magnetic field. This means that if one takes the resistive transition as in [23] the superconducting coherence length would be underestimated by a factor of 2.
- [39] A. A. Abrikosov and L. P. Gorkov, *Sov. Phys. JETP* **12**, 1243 (1961).